Published February 28, 2017

Phytate Degradation by Different Phosphohydrolase Enzymes: Contrasting Kinetics, Decay Rates, Pathways, and Isotope Effects

Mingjing Sun
Dep. of Plant and Soil Sciences
Univ. of Delaware
Newark, DE 19716

Jamal Alikhani
Arash Massoudieh
Civil Engineering Dep.
Catholic Univ. of America
Washington, DC 20064

Ralf Greiner
Dep. of Food Technology
and Bioprocess Engineering
Max Rubner-Institut
Federal Research Institute
of Nutrition and Food
76131 Karlsruhe
Germany

Deb P. Jaisi*
Dep. of Plant and Soil Sciences
Univ. of Delaware
Newark, DE 19716

Phytate (IP_6) is often the most common organic P compound particularly in agricultural soils. Understanding the fate of inositol phosphate (IP_x) in the environment in terms of isomeric composition and concentration and assessing relative resistance to (or preference for) degradation is essential to estimate the potential role of IP_x in generating inorganic P (P_i) as well as overall P cycling in the environment. In this study, we analyzed IP_6 degradation by four common phosphohydrolase enzymes (phytase from wheat [*Triticum aestivum* L.] and *Aspergillus niger* and acid phosphatase from wheat germ and potato [*Solanum tuberosum* L.]), with particular focus on degradation pathways, isomer kinetic decay rate, and isotope effects using a combination of high-performance ion chromatography, nuclear magnetic resonance, stable isotopes, and process-based modeling techniques. Our results show that the degradation pathways are often distinct among enzymes. The process-based Bayesian inverse modeling was used to capture the trend and magnitude of the measured concentrations for each IP_x isomer and to determine the decay constants. Furthermore, O isotope ratios ($\delta^{18}O_P$) of released P_i enabled the identification of isotopically identical phosphate moieties in phytate derived from natural sources. Distinctly different fractionation factors, degradation pathways, and kinetic decay rate coefficients among the enzymes studied could lead to potential discrimination and tracking of phytate sources and products as well as active enzymes present in the environment.

Abbreviations: HPIC, high-performance ion chromatography; IP, inositol phosphate; NMR, nuclear magnetic resonance; P_i, inorganic phosphorus; pNPP, *para*-nitrophenyl phosphate.

Core Ideas

- **Phytate is degraded through distinct pathways for a particular enzyme.**
- **Oxygen isotope ratios of phosphate moieties in phytate are isotopically identical.**
- **These findings bring new insights into tracking phytate sources in the environment.**

Inositol phosphates are a group of organic P compounds widely present in the natural environment (Turner et al., 2002). Phytate (the salt of *myo*-inositol 1,2,3,4,5,6-hexakisphosphate or IP_6) is a P storage molecule in cereals and grains and represents between 60 and 80% of P in mature seeds (Raboy, 1997). Since it is reported that ~51 million tonnes of phytate is formed in commercially produced fruits and crop seeds every year (Lott et al., 2000), a good fraction of phytate in seeds and grains is released to the soil environment as plant residues and animal manures (Dao, 2007; Gerke, 2015). Phytate readily sorbs onto minerals or precipitates with soil cations and organic matter, and then accumulates to constitute an often dominant class of organic P (Celi and Barberis, 2007; Giles and Cade-Menun, 2014). Although sorption and precipitation immobilizes a large fraction of phytate in soil, there is a potential for its transfer to water bodies with soil particulates and colloids (Turner et al., 2002; Turner and Newman, 2005). Because 1 mol of phytate contains 6 mol of phosphate, phytate degradation could

Soil Sci. Soc. Am. J. 81:61–75
doi:10.2136/sssaj2016.07.0219
Received 18 July 2016.
Accepted 17 Nov. 2016.
*Corresponding author (jaisi@udel.edu).

significantly increase inorganic P (P_i), and thus may contribute to eutrophication of coastal and freshwater resources (McKelvie, 2007), leading to a serious ecological concern.

Phytate is rather stable against abiotic degradation; however, it can quickly degrade in the presence of phytate-degrading enzymes (Cosgrove and Irving, 1980; Mullaney et al., 2007), which are widespread in the environment (Greiner, 2007; Konietzny and Greiner, 2002; Meek and Nicoletti, 1986; Shan et al., 1993). These enzymes can hydrolyze phytate and generate different inositol phosphate isomers (Greiner and Konietzny, 2011). The phytate numbering system follows D- and L- nomenclature (Fig. 1), which is not only for numbering the position of C atoms in the inositol but also for presenting the absolute stereochemistry structure of inositol phosphates (Shears and Turner, 2007). For instance, D-*myo*-inositol-1,4,5,6-tetrakisphosphate [D-I(1,4,5,6)P_4] and D-I(3,4,5,6)P_4 are a pair of enantiomers while D-I(1,3,4,5)P_4 and D-I(3,4,5,6)P_4 are positional isomers. The position of phosphate moieties on the inositol ring has been found to be related to physiological functions in cell biology, such as ion channel physiology, membrane dynamics, and nuclear signaling (Irvine and Schell, 2001). Different enzymes can remove the phosphate groups from different positions on the inositol ring and form low-order inositol isomers, of which positional isomers or enantiomers (Greiner et al., 2006) could be related to particular physiological functions (Blum-Held et al., 2001).

In the environment, the majority of P occurs as P_i and thus permits the use of stable isotope ratios of O in P_i ($\delta^{18}O_p$) as a potential tracer of P (Jaisi and Blake, 2014; Jaisi et al., 2014; McLaughlin et al., 2013). Organophosphorus compounds can be hydrolyzed by extracellular phosphatases or other enzymes and subsequently release P_i. In the case of enzymatic degradation of phytate, cleavage of a P–O bond linked to the inositol ring incorporates one O from water and inherits three O atoms from the parent phytate molecule in the released P_i (von Sperber et al., 2015; Wu et al., 2015). Because the generated P_i partially retains the isotope signature of the original phytate, there is a possibility to apply O isotope ratios to trace sources as well as track the fate of phytate in the environment. The aims of this research were: (i) to determine the enzymatic hydrolyzability of phytate by four common phosphohydrolase enzymes (phytase from wheat and *Aspergillus niger* and acid phosphatase from wheat germ and potato), (ii) to investigate the difference in the mechanisms and pathways of degradation among these enzymes, (iii) to compare the kinetic decay rate of different isomers of inositol phosphates, and (iv) to identify the O isotope effects of different enzymes. These aims were realized by running a series of enzymatic phytate degradation experiments and analyzing the inositol phosphate isomers generated by using high-performance ion chromatography (HPIC), nuclear magnetic resonance (NMR), and stable isotopes and by developing Bayesian inverse modeling to identify degradation constants for each isomer. We anticipate that a suite of information generated from these measurements will be useful for tracking the original source of phytate from its dephosphorylated products in the environment.

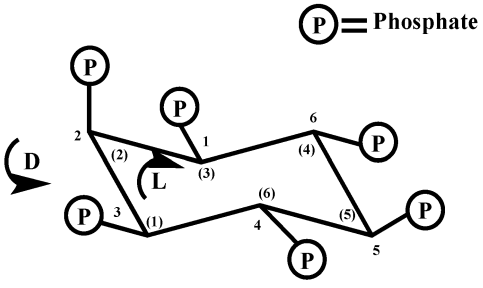

Fig. 1. Chemical structure of phytate. The configuration is assigned D when the numbering is counterclockwise and the configuration is L when clockwise.

MATERIALS AND METHODS

Chemicals and Reagents

Potassium phytate (a synthetic product), sodium phytate (from rice [*Oryza sativa* L.]), D-glucose-6-phosphate (G-6-P), and α-D-glucose-1-phosphate (G-1-P) were purchased from Sigma-Aldrich. Sodium pyrophosphate ($Na_4P_2O_7$) and *para*-nitrophenyl phosphate (pNPP) were obtained from Fisher Scientific. Similarly, phytase from wheat and acid phosphatases from potato and wheat germ were also obtained from Sigma-Aldrich, but phytase from *Aspergillus niger* (Natuphos) was kindly provided by BASF. Sources of other inositol phosphate standards are as follows: D-*myo*-inositol 1,2,4,5,6-pentakisphosphate, D-*myo*-inositol 1,2,3,4,6-pentakisphosphate, *myo*-inositol 1,3,4,6-tetrakisphosphate, L-*myo*-inositol 1,4,5-trisphosphate, D-*myo*-inositol 4,5-diphosphate, and *myo*-inositol 2-monophosphate from Sigma-Aldrich; D-*myo*-inositol 1,3,4,5,6-pentakisphosphate, D-*myo*-inositol 1,2,5,6-tetrakisphosphate, D-*myo*-inositol 1,4,5,6-tetrakisphosphate, D-*myo*-inositol 1,3,4,5-tetrakisphosphate, D-*myo*-inositol 1,2,4,5-tetrakisphosphate, D-*myo*-inositol 1,2,6-triphosphate, D-*myo*-inositol 1,5,6-triphosphate, D-*myo*-inositol 1,2-diphosphate, and D-*myo*-inositol 1-monophosphate from Cayman Chemical Company; and D-*myo*-inositol 1,2,3,5,6-pentakisphosphate and *myo*-inositol 1,2,3,6-tetrakisphosphate from Enzo Life Sciences. All assay reagents were prepared in double-deionized water.

Enzyme Purification and Hydrolyzability Assay

Because crude phytase enzyme from wheat contains a large amount of P_i and potentially other proteins and enzyme impurities (von Sperber et al., 2015; Wu et al., 2015), it was purified following the Brejnholt et al. (2011) method. Briefly, 15 g of crude phytase was dissolved with 0.1 M NaOAc (pH 4.3). After removing precipitates and insoluble impurities by centrifugation, the supernatant was collected and the protein was precipitated with 30% saturated $(NH_4)_2SO_4$ solution. It was precipitated again with 60% saturated $(NH_4)_2SO_4$. Precipitates were separated and dissolved in 0.1 M NaOAc and then purified by a HiTrap SP cation exchange column (GE Healthcare). The fractions containing a phytate-degrading enzyme (with an approximate molecular weight of 60 kDa) were pooled and further purified by a

HiTrap Q anion exchange column (GE Healthcare). After purification, the fraction was collected and run on a polyacrylamide gel (ThermoFisher Scientific) to identify the size of the protein bands. The enzyme activity was tested with phytate, and high-activity fractions were pooled, dialyzed against 0.1 M NaOAc buffer (pH 5.4), and then stored at −20°C.

For the enzyme activity assay, crude and purified wheat phytases (10 μL each) were added to 1 mL of 1 mM K phytate solution in 0.1 M NaOAc buffer (pH 5.4). The control experiment was performed in the same buffer but without the enzyme. After incubating at 55°C for 30 min, the reaction was stopped by adding an equal volume of 1 M HCl (Adeola et al., 2004). The amount of P_i released was measured by using the phosphomolybdate blue method (Murphy and Riley, 1962). Total protein content was determined by using the BCA Protein Assay Kit (ThermoFisher Scientific).

To determine the substrate selectivity, the activity of crude and purified wheat phytase enzymes to several phosphorylated compounds was tested. Briefly, 10 μL of phytase was incubated separately with 1 mL of 3 mM each of pNPP, G-6-P, G-1-P, and $Na_4P_2O_7$ in 0.1 M NaOAc buffer at pH 5.4 and 55°C. The reaction was stopped, and the released P_i was measured as described above. Similarly, the activity and substrate selectivity of *A. niger* phytase were tested by adding 10 μL of 1 mg mL^{-1} enzyme into 1 mM potassium phytate or 3 mM each of pNPP, $Na_4P_2O_7$, G-6-P, and G-1-P solution at pH 5.4 in NaOAc buffer. The experiments were incubated at 37°C for 30 min, and the released P_i was measured as above.

The activity of acid phosphatases was also tested. Briefly, 10 μL of 10 mg mL^{-1} enzyme was added to 1 mM potassium phytate or 3 mM other substrates at pH 5.4, incubated at 37°C for 30 min, and then the released P_i was quantified to calculate the enzyme activity. The activity of each enzyme is expressed in units (U): for wheat and *A. niger* phytase enzymes, 1 U will liberate 1 μmol P_i min^{-1} from phytate; for acid phosphatase from wheat germ and potato, 1 U will liberate 1 μmol P_i min^{-1} from pNPP. In terms of purity, wheat and *A. niger* phytase enzyme preparations are expected to contain a single phytate-degrading enzyme. However, because acid phosphatase from wheat germ and potato were crude extracts and no further purification was done, these enzymes might have contained more than one phytate-degrading enzyme and other phosphatase enzymes.

Phytate Degradation Experiments

Two sources of phytates were used as substrates in the degradation experiments: Na phytate (extracted from rice) and K phytate (a synthetic, pure product). After initial pilot enzyme activity tests, a series of experiments on the enzymatic degradation of phytate was performed using 1 U (0.005 U $μmol^{-1}$ phytate) purified wheat phytase in 200 mL of 1 mM K phytate solution at pH 5.4. All experiments were performed in 0.1 M NaOAc buffer and incubated at 55°C for optimal wheat phytase activity. For *A. niger* phytase, K phytate and Na phytate were used as substrates. The incubation experiments included 200 mL of 1 mM phytate solution (pH 5.4) in 1 U *A. niger* phytase at 37°C. For acid phosphatases from wheat germ and potato, 2 mM K phytate was incubated with different amounts of enzyme to achieve final enzyme activities of 0.2 and 3.2 U $μmol^{-1}$ phytate, respectively. All enzyme experiments were run in duplicate. The control experiment for each set of enzymes was performed under the same conditions but without enzymes.

Because of the different degradation kinetics among the enzymes studied, the timing for sampling was varied for each enzyme. For wheat phytase, *A. niger* phytase, and wheat germ acid phosphatase experiments, subsamples were collected every 15 min for the first 8 h, then every 2 h until 24 h, and then each day until 10 d. For the potato acid phosphatase experiments, subsamples were withdrawn at 0, 1, 2, 4, 8, 12 h, ..., until 10 d. At each time point, a 2-mL subsample was collected for HPIC and NMR analyses, and an additional 5- to 10-mL subsample was withdrawn (at selected time points only) for isotope analyses. An equal amount of 1 M HCl was added to stop the enzyme activity. For each sample, the amount of released P_i was quantified to monitor the progress of the degradation reaction.

For enzymes with slow phytate degradation kinetics, the stability of the enzymes was tested during incubation to ensure that the enzymes were not significantly deactivated. For this test, phytases (0.5 U) and acid phosphatases (1.5 U) were each incubated separately in 10 mL of 0.1 M NaOAc buffer (pH 5.4) at 37°C. Several subsamples were withdrawn at selected time points, and the residual enzyme activity was tested with phytate or pNPP substrate.

High-Performance Ion Chromatography Analysis

High-performance ion chromatography, the most appropriate technique to separate various inositol phosphate isomers, was used following the method of Chen and Li (2003). Briefly, a 1-mL collected sample was freeze-dried and redissolved in 0.5 mL of H_2O, filtered through a 0.2-μm filter disk, and then analyzed immediately. The separation was performed on a Dionex DX-500 ion chromatograph system, using a CarboPac PA-100 column under a gradient acidic eluent program. After post-column reaction with an Fe solution, the separated components were detected at 295 nm. An in-house reference standard was also prepared according to the Chen and Li (2003) method to identify different IP_x. Furthermore, a series of commercial IP_x standards (see above) was used to identity and quantify the degradation products.

Nuclear Magnetic Resonance Analysis

Phosphorus-31 NMR was used to identify isomers, particularly inositol monophosphates (IP_1), that could not be separated in HPIC. For selected samples, 1 mL of solution was freeze-dried and redissolved in 0.54 mL of 0.5 M NaOH and 0.06 mL D_2O, then transferred into a 5-mm NMR tube. Proton-coupled (512 scans) and decoupled (256 scans) ^{31}P NMR measurements were collected in an AV 600 MHz Bruker NMR spectrometer at the University of Delaware. Available IP_x isomer standards were also

analyzed to identify the NMR parameters for different degradation products.

Modeling of Degradation Kinetics

A process-based model and a Bayesian inverse model were used to determine the decay kinetics parameters of IP_x. The conceptual reaction network was developed by explicitly considering enzyme limitation and considering the fact that phosphohydrolase enzymes could have several active sites that are able to react with P centers on IP_x. This reaction was assumed to be sequential in that the removal of phosphate groups results in the reduction of the order of phytate from IP_n to IP_{n-1}:

$$E+\mathrm{IP}_{n,i}\rightarrow \mathrm{EP}+\mathrm{IP}_{n-1,j} \quad [1]$$

$$\mathrm{EP}\rightarrow E+P \quad [2]$$

where E is the available active sites on the enzyme molecule; $IP_{n,i}$ is the isomer of IP_n, with n being the number of P atoms on the molecule; and EP is the enzyme–P complex that is later broken down into the free enzyme (E) to release phosphate. The first reaction is the general degradation reaction where $IP_{n,i}$ loses one of its phosphate moieties and produces an $IP_{n-1,j}$ isomer. Assuming that $k_{n,i,j}$ is the rate constant for the reaction of $IP_{n,i}$ with the enzyme site to generate an $IP_{n-1,j}$ isomer, the general form of the governing equations controlling the kinetics of the chain transformations can be written as

$$\frac{\mathrm{d}[E]}{\mathrm{d}t}=-[E]\sum_{n=1}^{m}\sum_{i_1=1}^{l_m}\sum_{j_1=1}^{l_{m-1}}k_{n,i_1,j_1}\left[\mathrm{IP}_{n,i_1}\right]+k_{\mathrm{EP}}[\mathrm{EP}] \quad [3a]$$

$$\frac{\mathrm{d}\left[\mathrm{IP}_{n,i}\right]}{\mathrm{d}t}=[E]\left(\sum_{i_1=1}^{l_{n+1}}k_{n+1,i_1,j}\left[\mathrm{IP}_{n+1,j}\right]-\left[\mathrm{IP}_{n,i}\right]\sum_{j_2=1}^{l_n}k_{n,i,j_2}\right) \quad [3b]$$

$$\frac{\mathrm{d}[\mathrm{EP}]}{\mathrm{d}t}=[E]\sum_{n=1}^{m}\sum_{i_1=1}^{l_m}\sum_{j_1=1}^{l_{m-1}}k_{n,i_1,j_1}\left[\mathrm{IP}_{n,i_1}\right]-k_{\mathrm{EP}}[\mathrm{EP}] \quad [3c]$$

$$\frac{\mathrm{d}[\mathrm{P}]}{\mathrm{d}t}=k_{\mathrm{EP}}[\mathrm{EP}] \quad [3d]$$

where $k_{n,i,j}$ is the rate coefficient of the transformation of an isomer in IP_n to isomer j in IP_{n-1}, l_n is the number of possible isomers of IP_n, and m is the maximum number of phosphate moieties (or P atoms), which, for example, is six for IP_6. The recovery rate of the reacted enzyme site (EP) is assumed to be a first-order reaction, with the rate constant of k_{EP} as shown in Eq. [3d].

A Bayesian inference approach using the BIOEST program (Alikhani et al., 2017) was used to estimate the posterior probability distributions of all reaction rate coefficients as well as the initial P-equivalent concentrations of enzyme (E_0) defined based on the moles of IP molecules that can be involved (μM P equivalent). The Bayesian approach uses Markov chain Monte Carlo (MCMC) methods to sample from the posterior distribution based on a likelihood function calculated by assuming a lognormal and multiplicative error structure for the observed temporal variation of all isomers in each set of results. The benefit of using Bayesian inverse modeling, as opposed to the conventional deterministic parameter estimation, is not only that it informs us about the uncertainty associated with the parameter values but also assesses the non-uniqueness of parameters due to overparameterization of the reaction model.

Oxygen Isotope Ratios of Released Phosphate

To measure the O-isotope ratios of the released P_i ($\delta^{18}O_p$) during enzymatic degradation, 5- to 10-mL samples were purified using sequential precipitation and recrystallization methods described before (Jaisi and Blake, 2014). Silver phosphate (200–300 μg) in silver capsules, prepared in triplicate for each sample, was pyrolyzed in a thermochemolysis–elemental analyzer (TC–EA) at 1460°C. Oxygen isotope ratios were measured in an isotope ratio mass spectrometer (IRMS; Thermo). To measure O isotope ratios of intact phosphate moieties in phytate ($\delta^{18}O_{Po}$), 70 to 100 μg of freeze-dried phytate powder was pyrolyzed directly in TC–EA and measured by using IRMS. The raw isotope values were corrected using two silver phosphate standards, YR1-aR02 and YR3-2, with $\delta^{18}O_p$ values of −5.49 and 33.63‰, respectively.

For water O-isotope ($\delta^{18}O_W$) analysis, a 0.3-mL water sample was injected into airtight Exetainer tubes (Labco Limited) and equilibrated with 300 $cm^3\ m^{-3}$ CO_2 in He for 24 h (Upreti et al., 2015). After equilibration, the O-isotope ratios of CO_2 in the headspace were measured by IRMS. The $\delta^{18}O_W$ values were calculated from $\delta^{18}O_{CO2}$ values using a known fractionation factor ($\alpha_{CO2\text{-}H2O}$) (Cohn and Urey, 1938). The $\delta^{18}O_W$ values were calibrated with two water standards ($\delta^{18}O_W$ values of −1.97 and −9.25‰, USGS). All samples and standards for O-isotope ratios were run in duplicate. All isotope data are reported in per-mil (‰) values relative to Vienna standard mean ocean water.

The isotopic fractionation factors (F) of O between incorporated and ambient water during enzymatic phytate degradation was calculated from the measured $\delta^{18}O_{Po}$ and $\delta^{18}O_W$ (Liang and Blake, 2006) as

$$F=4\left(\delta^{18}O_p-0.75\,\delta^{18}O_{Po}\right)-\delta^{18}O_W \quad [4]$$

The fractionation factor calculated from this equation was used to compare differences among different enzymes and substrates.

RESULTS

Substrate-Specific Enzyme Activity

The activities of different enzymes to phytate are summarized in Table 1. As shown, wheat phytase enzyme activity was improved by ~50 times after purification. Interestingly, purified wheat phytase showed a broad substrate specificity. The relative activities toward pNPP, $Na_4P_2O_7$, and G-6-P compared with that of phytate were 200, 388, and 12%, respec-

Table 1. Enzyme activity of different phosphorylated compounds.

Compound†	Activity				
	Purified wheat phytase	Crude wheat phytase	*A. niger* phytase	Acid phosphatase (wheat germ)	Acid phosphatase (potato)
	U mg^{-1} protein			U mg^{-1} solid powder	
K phytate	0.50 ± 0.02	0.012 ± 0.002	13.49 ± 0.44	0.02 ± 0.006	0.002 ± 0.0005
pNPP	1.00 ± 0.21	0.082 ± 0.001	1.52 ± 0.13	0.37 ± 0.04	0.394 ± 0.04
$Na_4P_2O_7$	1.94 ± 0.39	0.194 ± 0.007	1.23 ± 0.27	0.70 ± 0.09	0.784 ± 0.14
G-6-P	0.06 ± 0.008	0.032 ± 0.009	0.25 ± 0.04	0.04 ± 0.004	0.042 ± 0.002
G-1-P	0.41 ± 0.09	0.096 ± 0.02	1.04 ± 0.32	0.10 ± 0.03	0.137 ± 0.05

† K phytate, potassium phytate; pNPP, *para*-nitrophenylphosphate; $Na_4P_2O_7$, sodium pyrophosphate; G-6-P, D-glucose-6-phosphate; G-1-P, α-D-glucose-1-phosphate.

tively. Nonetheless, these results are similar to those in previous studies (Greiner et al., 1998; Nagai and Funahashi, 1962). For *A. niger* phytase, the highest activity was observed with phytate (13.49 U mg^{-1}) and the relative activities to other substrates ranged from 2 to 11%.

For acid phosphatases from wheat germ and potato, activities to phytate were very low (0.02 and 0.002 U mg^{-1}). However, both acid phosphatases showed similar activities to the other substrates. The range of activities to the series of substrates studied (pNPP, $Na_4P_2O_7$, G-6-P, and G-1-P) varied from 0.04 to 0.78 U mg^{-1}.

Kinetics of Phytate Degradation Catalyzed by Different Enzymes

The kinetics of enzymatic degradation of phytate are shown in Fig. 2. Both purified wheat phytase and *A. niger* phytase could rapidly degrade phytate and achieved ~500% degradation in ~24 h (i.e., 5 mol of P_i were released from 1 mol of phytate), consistent with our recent study (Wu et al., 2015). Continued incubation showed no further release of P_i after 240 h, suggesting that these two phytases were unable to degrade inositol monophosphate. For acid phosphatase from wheat germ, the rate of degradation was comparable to that of phytase and could remove 5 phosphate moieties from the inositol ring. For acid phosphatase from potato, P_i release was slowest but achieved ~580% yield in 10 d.

Separate enzyme stability test results showed that the enzymes retained >80% of their original activity after 24 h of incubation, and the activity decreased gradually with time. For example, the residual enzyme activity at 240 h was 48% for *A. niger* phytase, 16% for wheat phytase, 56% for acid phosphatase from wheat germ, and 63% for acid phosphatase from potato. High residual enzyme activity in acid phosphatase suggests that slow degradation kinetics is not due to enzyme deactivation but rather the inability of the enzyme itself for rapid hydrolysis.

Identification of Degradation Products by High-Performance Ion Chromatography

Chromatograms of different IP_x compounds generated during enzymatic degradation of phytate are showed in Fig. 3, and their corresponding concentrations are presented in Fig. 4. Our results suggest a stepwise dephosphorylation of phytate via the formation of IP_5, IP_4, IP_3, and IP_2, but the isomeric composition of each IP_x varied. For wheat phytase, for example, at 4 h a significant decrease of IP_6 (~80%) occurred with a consequent increase of I(1,2,3,4,6)P_5 and D/L-I(1,2,3,4,5)P_5. A slight increase in D/L-I(1,2,4,5,6)P_5 was observed at this time but gradually decreased thereafter. Because the original phytate contained a small amount of D/L-I(1,2,4,5,6)P_5 as an impurity (see initial concentration at 0 h in Fig. 4A), the detected isomer could come both from impurities and also from IP_6 degradation. Furthermore, D/L-I(1,2,5,6)P_4 and D/L-I(1,2,3,4)P_4–I(1,3,4,6)P_4 co-eluted simultaneously: they appeared after 1 h, reached the maximum at about 6 h, and then started decreasing as the degradation continued. One IP_3 peak was also observed as early as ~4 h, which might contain co-eluted I(1,2,3)P_3–D/L-I(1,2,6)P_3–D/L-I(1,4,6)P_3, and reached

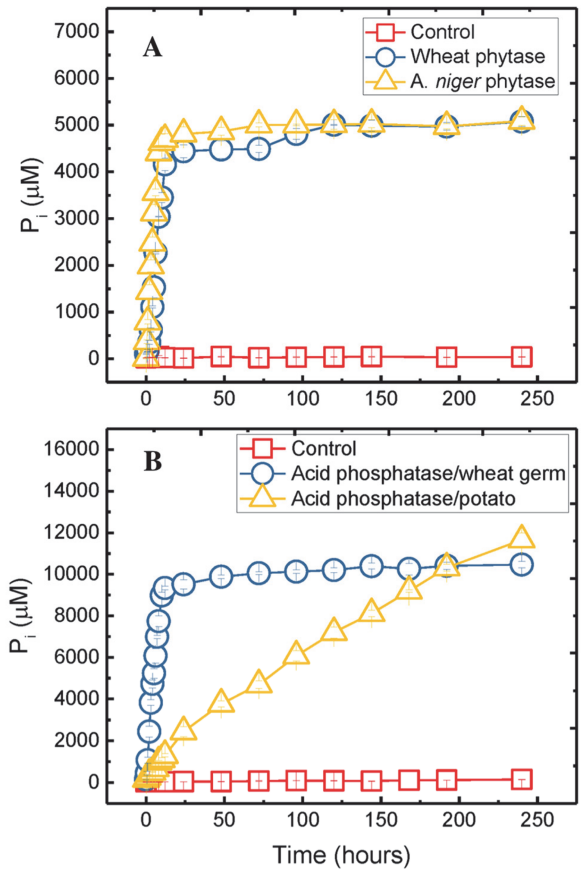

Fig. 2. Kinetics of phytate (as inorganic P, P_i) degradation catalyzed by four different enzymes.

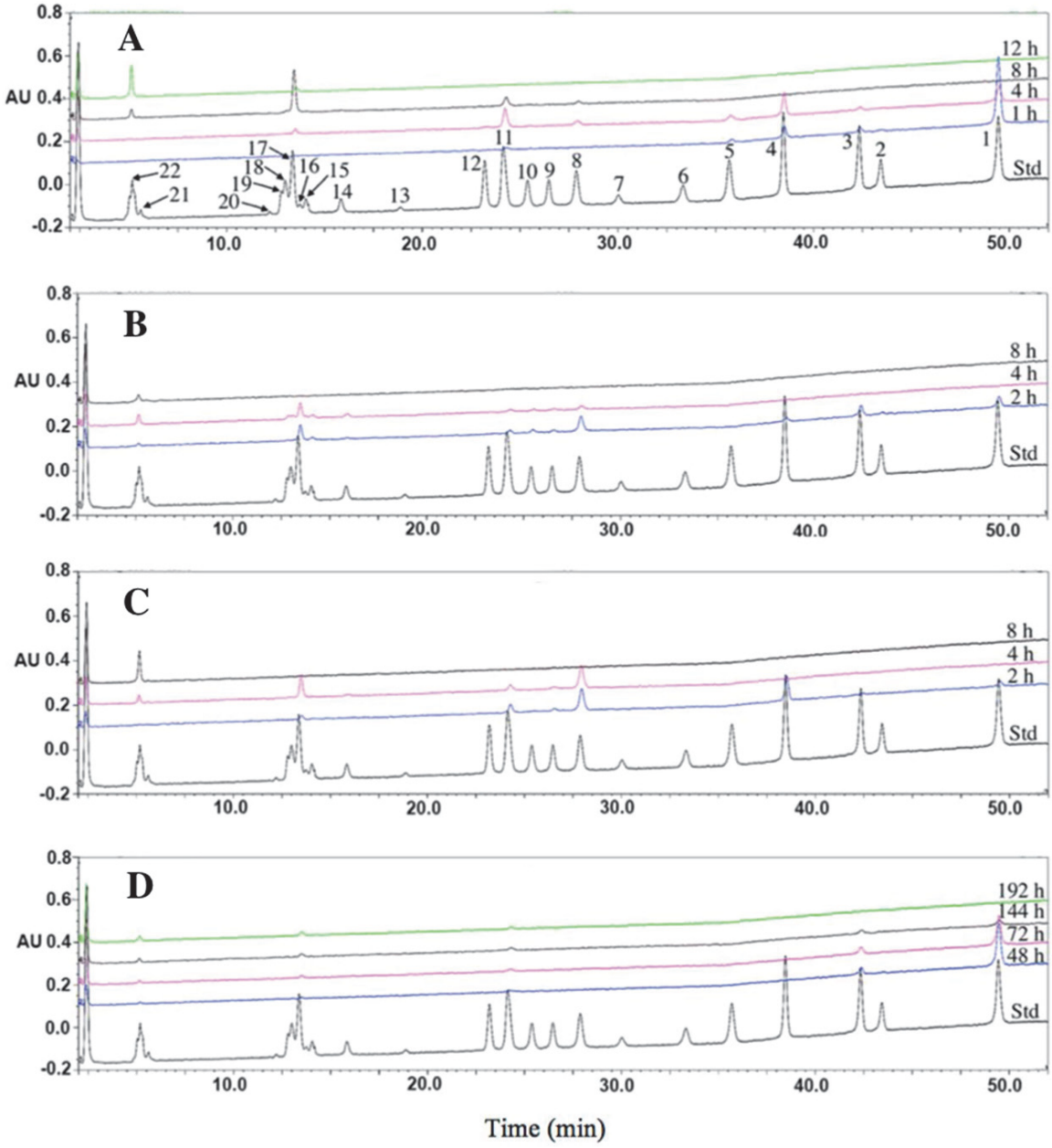

Fig. 3. Representative high performance ion chromatography (HPIC) chromatogram during phytate degradation by different enzymes: (A) wheat phytase; (B) *Aspergillus niger* phytase; (C) acid phosphatase from wheat germ; and (D) acid phosphatase from potato. Std: in-house reference standard. Peaks: (1) IP_6; (2) I(1,3,4,5,6)P_5; (3) D/L-I(1,2,4,5,6)P_5; (4) D/L-I(1,2,3,4,5)P_5; (5) I(1,2,3,4,6)P_5; (6) D/L-I(1,4,5,6)P_4; (7) I(2,4,5,6)P_4; (8) D/L-I(1,2,5,6)P_4; (9) D/L-I(1,3,4,5)P_4; (10) D/L-I(1,2,4,5)P_4; (11) D/L-I(1,2,3,4)P_4, I(1,3,4,6)P_4; (12) D/L-I(1,2,4,6)P_4, I(1,2,3,5)P_4; (13) I(4,5,6)P_3; (14) D/L-I(1,5,6)P_3; (15) D/L-I(2,4,5)P_3; (16) D/L-I(1,4,5)P_3; (17) I(1,2,3)P_3, D/L-I(1,2,6)P_3, D/L-I(1,4,6)P_3; (18) D/L-I(1,2,4)P_3, D/L-I(2,3,5)P_3; (19) D/L-I(1,3,4)P_3; (20) I(2,4,6)P_3; (21) D/L-I(4,5)P_2, I(2,5)P_2; (22) D/L-I(1,2)P_2.

maximum concentration at ~ 8 h. By 10 h of incubation, IP_3 also decreased and D/L-I(1,2)P_2 appeared as the dominant product. After 48 h of incubation, no additional isomers were observed (not shown). However, based on the degradation kinetics (Fig. 2), the D/L-I(1,2)P_2 could still be broken down to generate IP_1 isomers (see below for NMR results).

For *A. niger* phytase, the results are more complex because several lower order IP_x were detected early in the incubation (Fig. 4B). At the beginning, D/L-I(1,2,4,5,6)P_5 was the major IP_5 product, with small amounts of I(1,3,4,5,6)P_5 and D/L-I(1,2,3,4,5)P_5 isomers concurrently present. Concentrations of IP_5 increased first, reached their maximum in about 1 h, and then decreased. As IP_5 waned, IP_4 isomers appeared as major products. Four distinct IP_4 peaks were detected: D/L-I(1,2,5,6)P_4, D/L-I(1,3,4,5)$_4$, D/L-I(1,2,4,5)P_4, and D/L-I(1,2,3,4)P_4–I(1,3,4,6)P_4, with D/L-I(1,2,5,6)P_4 being the dominant product. Five IP_3 isomer peaks were observed as the degradation progressed: the major isomers included I(1,2,3)P_3–D/L-I(1,2,6)P_3–D/L-I(1,4,6)P_3 (co-eluted), and small amounts of D/L-(1,5,6)P_3, D/L-(2,4,5)P_3, D/L-I(1,2,4)P_3–D/L-I(2,3,5)P_3 (co-eluted), and D/L-I(1,3,4)P_3. The identity of the IP_2 isomer was determined to be D/L-I(1,2)P_2 from the authentic standard. This isomer appeared at ~2 h and disappeared completely by ~48 h of incubation. There might be additional IP_2 isomers in the product based

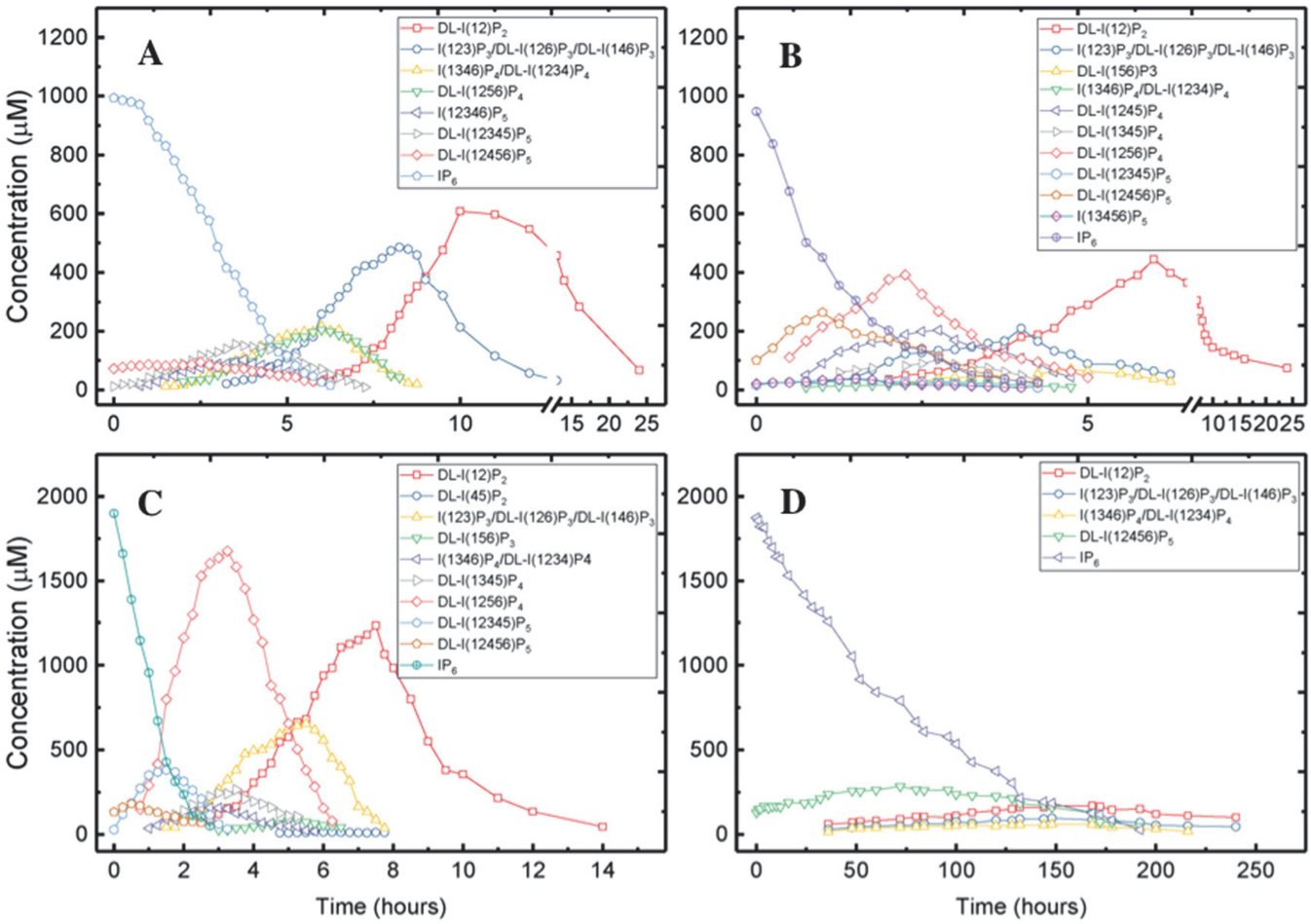

Fig. 4. Formation of various IP_x isomers during enzymatic phytate degradation based on the high performance ion chromatography results (Fig. 3): (A) wheat phytase; (B) *Aspergillus niger* phytase; (C) acid phosphatase from wheat germ; and (D) acid phosphatase from potato. Please note that each data point is a separately measured datum from subsamples collected during degradation.

on the fact that D/L-I(1,2)P_2 is not necessarily the sole degradation product of all IP_3 isomers. It is likely that the concentrations of other IP_2 isomers were too low to be detected.

For acid phosphatase preparation from wheat germ, the HPIC results were comparable to that of wheat phytase but with several unique differences (Fig. 4C). First, D/L-I(1,2,3,4,5)P_5 and D/L-I(1,2,4,5,6)P_5 were generated and D/L-I(1,2,3,4,5)P_5 was the major IP_5 accumulated during the early stage of degradation. Then, three IP_4 isomers appeared: D/L-I(1,2,5,6)P_4, D/L-I(1,3,4,5)P_4, and D/L-I(1,2,3,4)P_4–I(1,3,4,6)P_4, of which D/L-I(1,2,5,6)P_4 was about eight times higher in concentration than the other two isomers. Later, two IP_3 isomer peaks were observed: (1,2,3)P_3–D/L-I(1,2,6)P_3–D/L-I(1,4,6)P_3 and D/L-I(1,5,6)P_3. The final product, D/L-I(1,2)P_2, accumulated for a long time before it disappeared in ~16 h.

Unlike the other three enzymes, acid phosphatase preparation from potato hydrolyzed phytate very slowly (Fig. 4D). As a result, released IP_x isomers were present for a longer time. For example, D/L-I(1,2,4,5,6)P_5 did not disappear until 176 h. With progress in degradation, three additional peaks of IP_x isomers were detected: D/L-I(1,2,3,4)P_4–I(1,3,4,6)P_4, I(1,2,3)P_3–D/L-I(1,2,6)P_3–D/L-I(1,4,6)P_3, and D/L-I(1,2)P_2. A very small peak of I(1,3,4,5,6)P_5 was also observed in several samples. All isomers were present in very low concentration.

Overall, the HPIC results allowed discrimination of IP_2 to IP_6 isomers among the different enzymes.

Identification of Inositol Monophosphates by Nuclear Magnetic Resonance Spectroscopy

The NMR analysis of K phytate showed four characteristic peaks with a 1:2:2:1 peak area ratio, which is consistent with the symmetry rule (Fig. 1) and reported in the literature (e.g., Wu et al., 2015). The NMR results from wheat phytase (Fig. 5A) showed the emergence of several distinct peaks that belonged to a particular IP_x. With continued incubation, the amount of P_i increased at the expense of IP_x peaks, as expected and consistent with the HPIC results. The appearance of IP_1 was observed later in the incubation, suggesting that wheat phytase can dephosphorylate two phosphate groups both linked to D/L-I(1,2)P_2. However, IP_1 isomers could not be degraded any further, which confirmed that only five (out of six) phosphate moieties in the phytate molecule were released, with IP_1 being the final degradation product. Based on the distinct chemical shift and proton coupling parameter ($^3J_{1H,31P}$) of two commercially available IP_1 (Table 2), the exact compo-

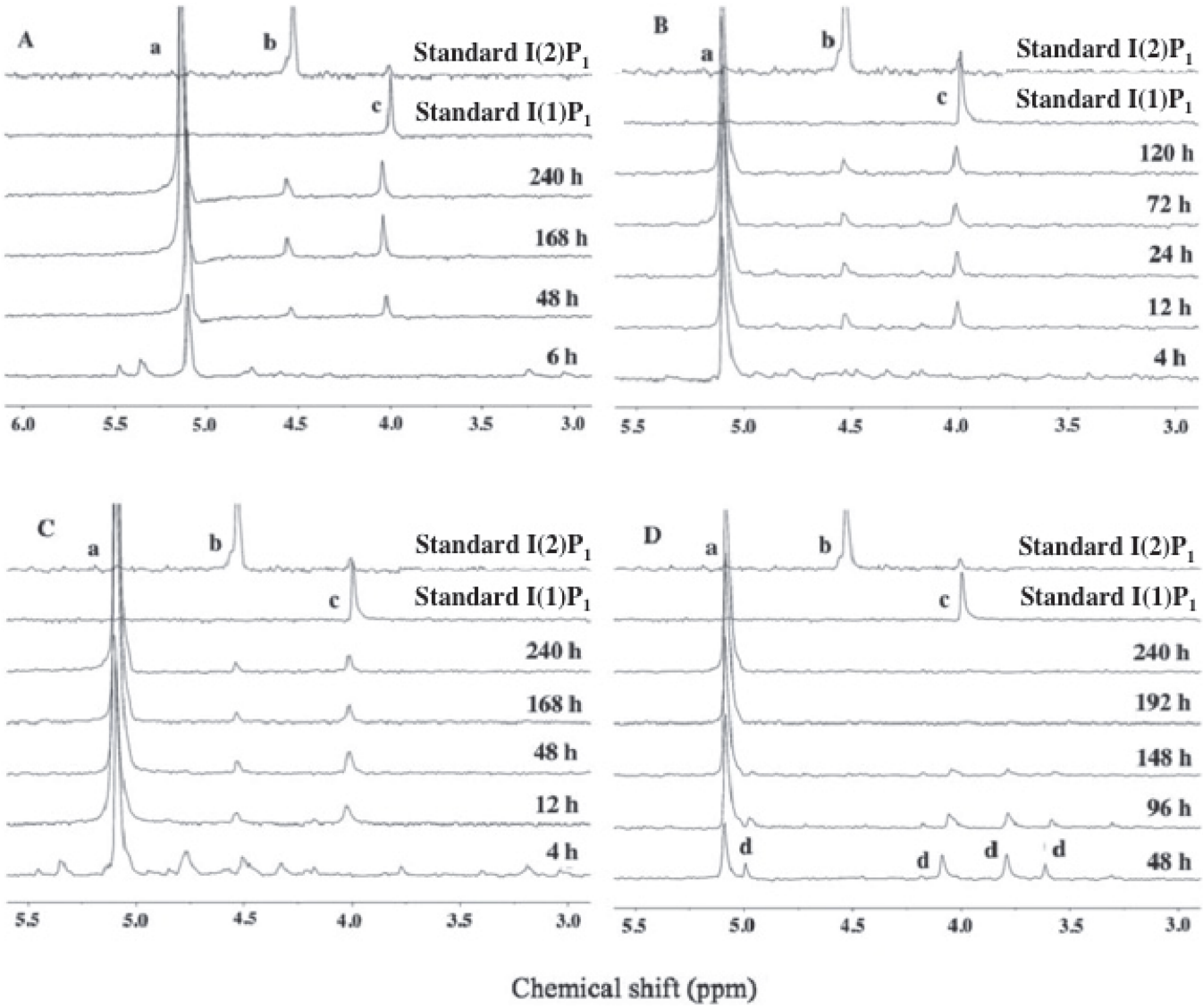

Fig. 5. Representative ^{31}P nuclear magnetic resonance spectra during phytate degradation by different enzymes: (A) wheat phytase; (B) *Aspergillus niger* phytase; (C) acid phosphatase from wheat germ; and (D) acid phosphatase from potato. Labeled peaks: (a) inorganic P (P_i), (b) I(2)P_1, (c) I(1)P_1, (d) phytate.

sitions of the IP_1 isomers were identified as I(2)P_1 and I(1)P_1. Interesting, the peak area ratio of I(2)P_1 to I(1)P_1 was around 1:1.9 at the end of the incubation with wheat phytase, suggesting that this enzyme preferably releases a phosphate moiety from the C-2 position.

Aspergillus niger phytase and acid phosphatase from wheat germ degraded D/L-I(1,2)P_2 isomers to I(2)P_1 and I(1)P_1, and both of them were retained during the entire incubation period as final products (Fig. 5B and 5C). The peak area ratios of I(2)P_1 to I(1)P_1 for *A. niger* phytase and acid phosphatase from wheat germ were around 1:1.4 and 1:1.8, respectively. For acid phosphatase from potato, phytate degradation was much slower (Fig. 5D) but the yield was >500% (Fig. 2B). Considering that this enzyme could release more than five phosphate groups and D/L-I(1,2)P_2 was detected by HPIC, we anticipated that there might be some further degradation products from IP_2. However, none of the IP_x isomers were detected besides phytate during the whole incubation period. Nonetheless, for the other three enzymes, IP_1 detected as final products by NMR were consistent with the results from the kinetic study in that five phosphate moieties were released from the inositol ring.

Table 2. The 31P nuclear magnetic resonance (NMR) parameters for phytate and inositol monophosphate standards. Chemical shifts, coupling constants, and peak area ratios were used to identify phytate degradation products by ^{31}P NMR reported in Fig. 5.

Inositol phosphates	Peaks	Peak area ratio	Chemical shift	$^3J_{1H,31P}$ constant
	no.		ppm	Hz
Potassium phytate	4	1:2:2:1	5.17;4.28;3.91;3.77	11.7;10.1;11.5;11.8
D-*myo*-inositol-1-monophosphate	1	–	3.99	8.3
myo-inositol-2-monophosphate	1	–	4.53	7.3

Table 3. Stoichiometric and rate expressions (Peterson matrix) for the enzymatic decay of wheat phytase.

Reaction	IP_6	$I(12456)P_5$	$I(12356)P_5$	$I(12346)P_5$	$I(1256)P_4$	$I(1236)P_4$	IP_3	IP_2	$P+IP_1$	E†	EP‡	Process rate§
1	−1	5/6								−1/6	1/6	$k_{P6,12456}$. E. IP_6
2	−1		5/6							−1/6	1/6	$k_{P6,12356}$. E. IP_6
3	−1			5/6						−1/6	1/6	$k_{P6,12346}$. E. IP_6
4		−1			4/5					−1/5	1/5	$k_{12456,1256}$. E.$I_{(12456)}P_5$
5			−1		4/5					−1/5	1/5	$k_{12356,1256}$. E. $I_{(12356)}P_5$
6			−1			4/5				−1/5	1/5	$k_{12356,1236}$. E. $I_{(12356)}P_5$
7				−1		4/5				−1/5	1/5	$k_{12346,1236}$. E. $I_{(12346)}P_5$
8					−1		3/4			−1/4	1/4	$k_{1256,126}$. E. $I_{(1256)}P_4$
9						−1	3/4			−1/4	1/4	$k_{1236,123}$. E. $I_{(1236)}P_4$
10							−1	2/3		−1/3	1/3	$k_{p3,p2}$. E. IP_3
11								−1	1/2	−1/2	1/2	$k_{p2,p1}$. E. IP_2
12									1	1	−1	k_{EP}. EP

† E is the available active sites on the enzyme molecule.

‡ EP is the enzyme–P complex.

§ $k_{n,n-1}$ is the rate coefficient of transformation from IP_n to IP_{n-1}.

Modeling of Degradation Kinetics

The stoichiometric and rate expression (Peterson matrix) for the reaction network (Eq. [3a–3d]) for wheat phytase degradation is shown in Table 3. The estimated expected values and standard deviations of the reaction parameters for the three enzymes are summarized in Table 4. As expected from the HPIC data (Fig. 4), the kinetic decay rate coefficients varied significantly among IP_x isomers. For example, the coefficient for IP_2 degradation to IP_1 was the lowest for all isomers, with *A. niger* phytase showing the lowest coefficient among enzymes included in the model. For most of the parameters, the standard deviations representing a measure of uncertainty are reasonably small compared with the mean, indicating relatively strong confidence in the parameter values and a lack of non-identifiability.

Figure 6 shows the observed and 95% credible interval for the predicted IP_x concentrations from wheat phytase. The results show good agreement between modeled and observed IP_x isomers. Similar results were obtained for *A. niger* phytase and acid phosphatase (wheat germ) but are not shown here for the sake of brevity. The modeling results are indicative of enzyme concentration being the limiting factor on the overall rate of the decay process. This is also evident from the mostly linear trends in the declining limbs of almost all IP_x.

Isotopic Composition of Released Orthophosphate from Phytate Degradation

Released orthophosphate analyzed for O-isotope composition during stepwise degradation of phytate by different enzymes showed interesting results (Fig. 7). During the entire incubation period, the measured $\delta^{18}O_p$ values were found to be almost constant, with the average isotope values of 16.78 ± 0.38‰ and 16.77 ± 0.58‰ for P_i released from Na phytate and K phytate degraded by *A. niger* phytase, respectively (see Table 5). For the other three enzymes, the measured $\delta^{18}O_p$ values of P_i released from K phytate were as follows: 14.88 ± 0.39‰ for wheat phytase, 15.22 ± 0.36‰ for acid phosphatase from wheat germ, and 16.12 ± 0.54‰ for acid phosphatase from potato.

Fractionation factors among the different enzymes, calculated from Eq. [1], were distinctly different (Table 5). For example, wheat phytase and acid phosphatase from wheat germ both have low fractionation factors compared with *A. niger* phytase and acid phosphatase from potato. A unique dif-

Table 4. Estimated mean and standard deviation for the kinetic decay rate coefficients obtained from Bayesian inverse modeling.

	Wheat phytase		*A. niger* phytase		Acid phosphatase (wheat germ)	
Parameter†	Mean	SD	Mean	SD	Mean	SD
	(h μM)$^{-1}$					
$k_{P6,13456}$	–	–	6.93	0.43		
$k_{P6,12456}$	95.80	7.39	47.05	1.39	17.34	4.37
$k_{P6,12356}$	48.30	4.31	4.65	0.34	103.33	18.68
$k_{P6,12346}$	34.15	3.68	–	–	–	–
$k_{13456,1345}$	–	–	97.03	4.85	–	–
$k_{12456,1245}$	–	–	38.94	1.70	–	–
$k_{12456,1256}$	176.88	18.49	61.49	2.98	125.88	28.72
$k_{12356,1236}$	100.20	12.22	52.90	3.77	12.15	2.82
$k_{12356,1256}$	19.17	4.67	–	–	41.92	7.85
$k_{12346,1236}$	124.55	15.77	–	–	–	–
$k_{12356,1356}$	–	–	–	–	5.81	1.17
$k_{1345,134}$	–	–	31.32	1.72	–	–
$k_{1356,156}$	–	–	–	–	5.65	1.80
$k_{1245,245}$	–	–	29.19	2.78	–	–
$k_{1245,124}$	–	–	1.83	0.15	–	–
$k_{1256,156}$	–	–	8.08	0.56	0.63	0.15
$k_{1256,126}$	39.92	5.55	27.68	1.26	5.66	1.00
$k_{1236,126}$	67.49	7.24	28.82	2.72	2.00	0.63
$k_{1236,123}$	–	–	26.26	1.95	12.33	2.02
$k_{245,12}$	–	–	46.61	4.61	–	–
$k_{124,12}$	–	–	155.07	11.11	–	–
$k_{156,56}$	–	–	6.13	0.57	9.93	3.89
$k_{126,12}$	15.09	1.64	22.54	1.74	17.01	4.88
$k_{123,12}$	–	–	16.43	1.42	0.75	0.20
$k_{56,P1}$	–	–	–	–	10.50	0.61
$k_{12,P1}$	0.036	0.0063	0.0052	0.0005	0.012	0.0021
k_{EP}, h^{-1}	59.52	8.33	16.29	0.64	21.44	3.21

† $k_{n,n-1}$ is the rate coefficient of transformation from IP_n to IP_{n-1}.

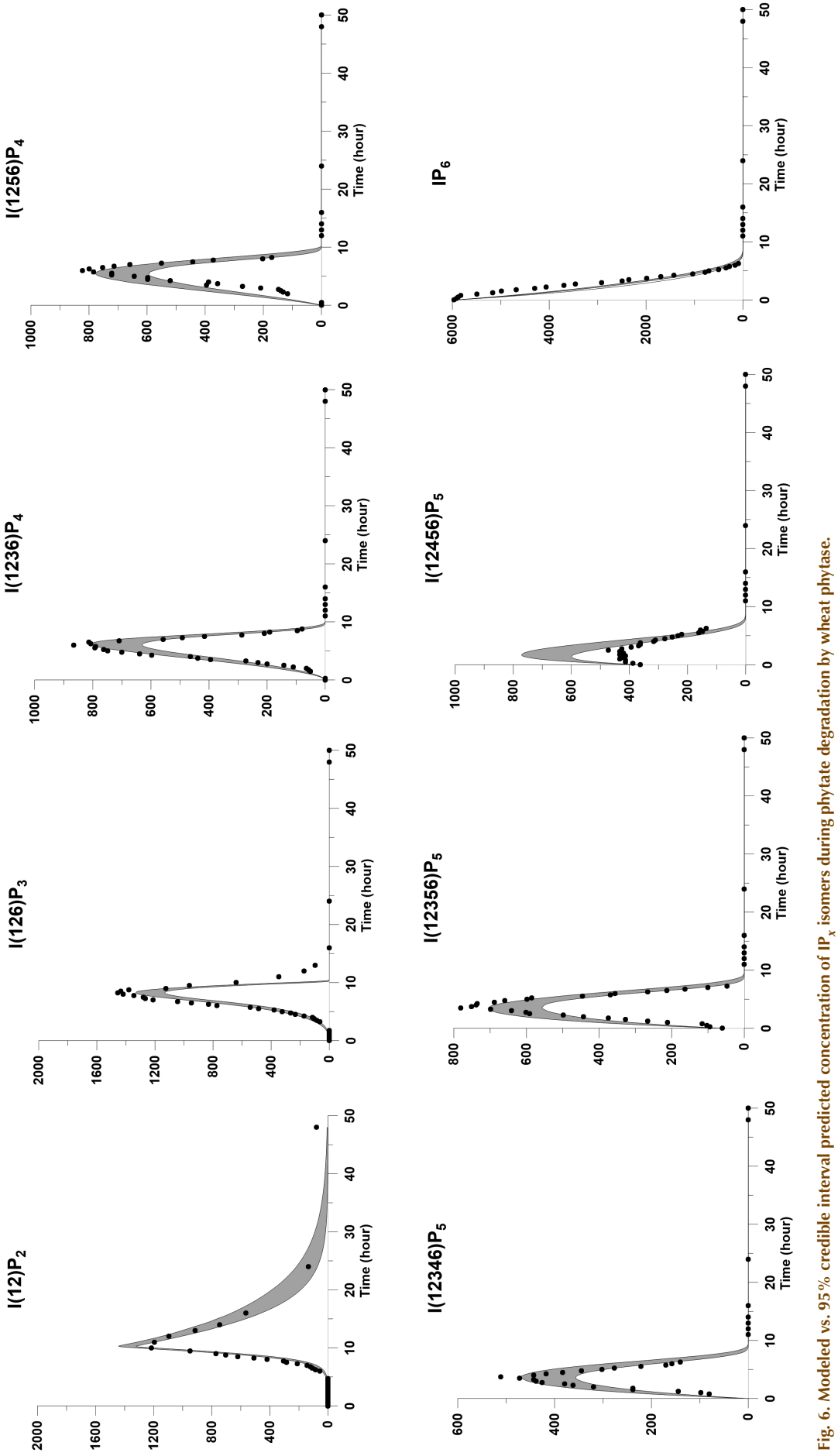

Fig. 6. Modeled vs. 95% credible interval predicted concentration of IP_x isomers during phytate degradation by wheat phytase.

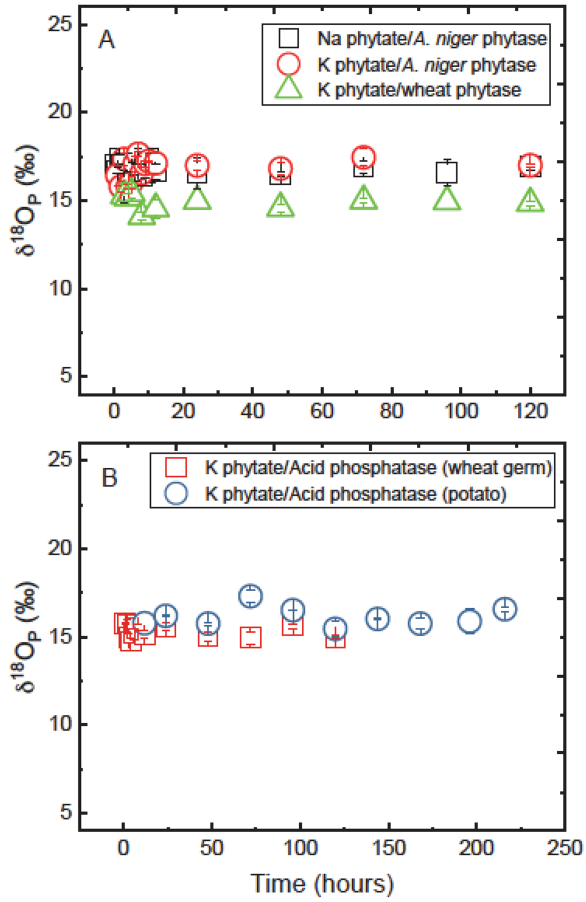

Fig. 7. The phosphate O-isotope ratios ($\delta^{18}O_P$) of inorganic P (P_i) accumulated at different time points during progressive degradation of Na phytate and K phytate.

ference for phytate, however, compared with other organic P compounds (e.g., Jaisi et al., 2014) is that *F* is positive for all enzymes studied and is within the range of published results (von Sperber et al., 2015; Wu et al., 2015).

DISCUSSION

Major and Minor Pathways of Phytate Degradation

Phytate-degrading enzymes from different sources differ in their specificity as well as their extent of phytate degradation (Greiner et al., 2000; Wyss et al., 1999). Generally, all enzymes that are capable of dephosphorylating phytate are defined as *phytase*. Depending on the stereochemical position in phytate at which a P–O bond is initially attacked, the enzymes are classified into three groups: (i) 3-phytase (EC 3.1.3.8), which hydrolyzes a P–O bond first from the D-3 or L-3 position, (ii) 6-phytase (EC 3.1.3.26), which preferentially initiates P–O bond cleavage at the L-6 (D-4) or D-6 position, and (iii) 5-phytase (EC 3.1.3.72), initiating phytate degradation at the D-5 position (Barrientos et al., 1994; Greiner and Alminger, 2001; Greiner et al., 1997, 2000; Konietzny and Greiner, 2002). Because of the positional selectivity of each enzyme, they could have distinct degradation kinetics and generate distinct pathways. This distinction could provide an avenue to identify the original sources of phytate in the environment.

Based on the results obtained from HPIC and ^{31}P NMR analyses (Fig. 4 and 5), potential degradation pathways for four different enzymes were generated and are summarized in Fig. 8 and 9. It is noteworthy to mention that enzyme selectivity provides additional information useful to ascertain a particular isomer. For wheat phytase, for example, D/L-I(1,2,3,4,5)P_5 [equivalent to D/L-I(1,2,3,5,6)P_5] was detected as the major IP_5 isomer at the initial stage of degradation. Because wheat phytase is a 6-phytase, D/L-I(1,2,3,4,5)P_5 should be D-I(1,2,3,5,6)P_5 with a phosphate group released from the D-4 position (Lim and Tate, 1973; Nakano et al., 2000). This also narrows down the possibilities of further dephosphorylation products from D-I(1,2,3,5,6)P_5. There were two other less significant IP_5 isomers detected during phytate degradation: D/L-I(1,2,4,5,6)P_5 [equivalent to D/L-I(2,3,4,5,6)P_5] and I(1,2,3,4,6)P_5. As shown, there is one major and two minor degradation pathways for wheat phytase: the major pathway proceeds via D-I(1,2,3,5,6)P_5, D-I(1,2,3,6)P_4, and D-I(1,2,5,6)P_4, I(1,2,3)P_3–D-I(1,2,6)P_3, D/L-I(1,2)P_2, and finally into I(2)P_1 and D/L-I(1)P_1. This pathway of degradation is consistent with published results (Chen and Li, 2003; Nakano et al., 2000). One minor route proceeds via D/L-I(1,2,4,5,6)P_5, D/L-I(1,2,5,6)P_4, D/L-I(1,2,6)P_3, D/L-I(1,2)P_2, I(2)P_1, and then to D/L-I(1)P_1, similar to our previous study (Wu et al., 2015). Another possible minor pathway proceeds via I(1,2,3,4,6)P_5, D/L-I(1,2,3,6)P_4, and/or D/L-I(1,3,4,6)P_4, I(1,2,3)P_3–D/L-I(1,2,6)P_3, and/or D/L-I(1,4,6)P_3, D/L-I(1,2)P_2, I(2)P_1, and then D/L-I(1)P_1. Compositions of some of the lower order dephosphorylation products are not included because they require further confirmation (Fig. 8A).

For acid phosphatase extracted from wheat germ, one major and one minor pathway of degradation were established (Fig. 8B). The IP_5 product identified as D/L-I(1,2,3,4,5)P_5 was confirmed to be D-I(1,2,3,5,6)P_5 for the major pathway, which then further degraded to generate four IP_4, among which

Table 5. Isotopic composition of released phosphate from K-phytate, including the O-isotope ratio of intact phosphate moieties from K-phytate ($\delta^{18}O_{Po}$), the O-isotope ratio of water ($\delta^{18}O_W$), and the O-isotope ratio of released inorganic P ($\delta^{18}O_P$), and O fractionation factors (*F*) in the reactions catalyzed by different enzymes.

Enzymes	Substrate	$\delta^{18}O_{Po}$	$\delta^{18}O_W$	$\delta^{18}O_P$	*F*
		‰			
A. niger phytase	Na phytate	19.75 ± 0.19	−7.02 ± 0.04	16.78 ± 0.38	14.91 ± 1.53
A. niger phytase	K phytate	20.53 ± 0.22	−7.02 ± 0.04	16.77 ± 0.58	12.50 ± 2.33
Wheat phytase	K phytate	20.53 ± 0.22	−7.02 ± 0.04	14.88 ± 0.39	4.78 ± 1.54
Acid phosphatase (wheat germ)	K phytate	20.53 ± 0.22	−7.02 ± 0.04	15.22 ± 0.36	6.15 ± 1.35
Acid phosphatase (potato)	K phytate	20.53 ± 0.22	−7.02 ± 0.04	16.12 ± 0.54	10.05 ± 2.25

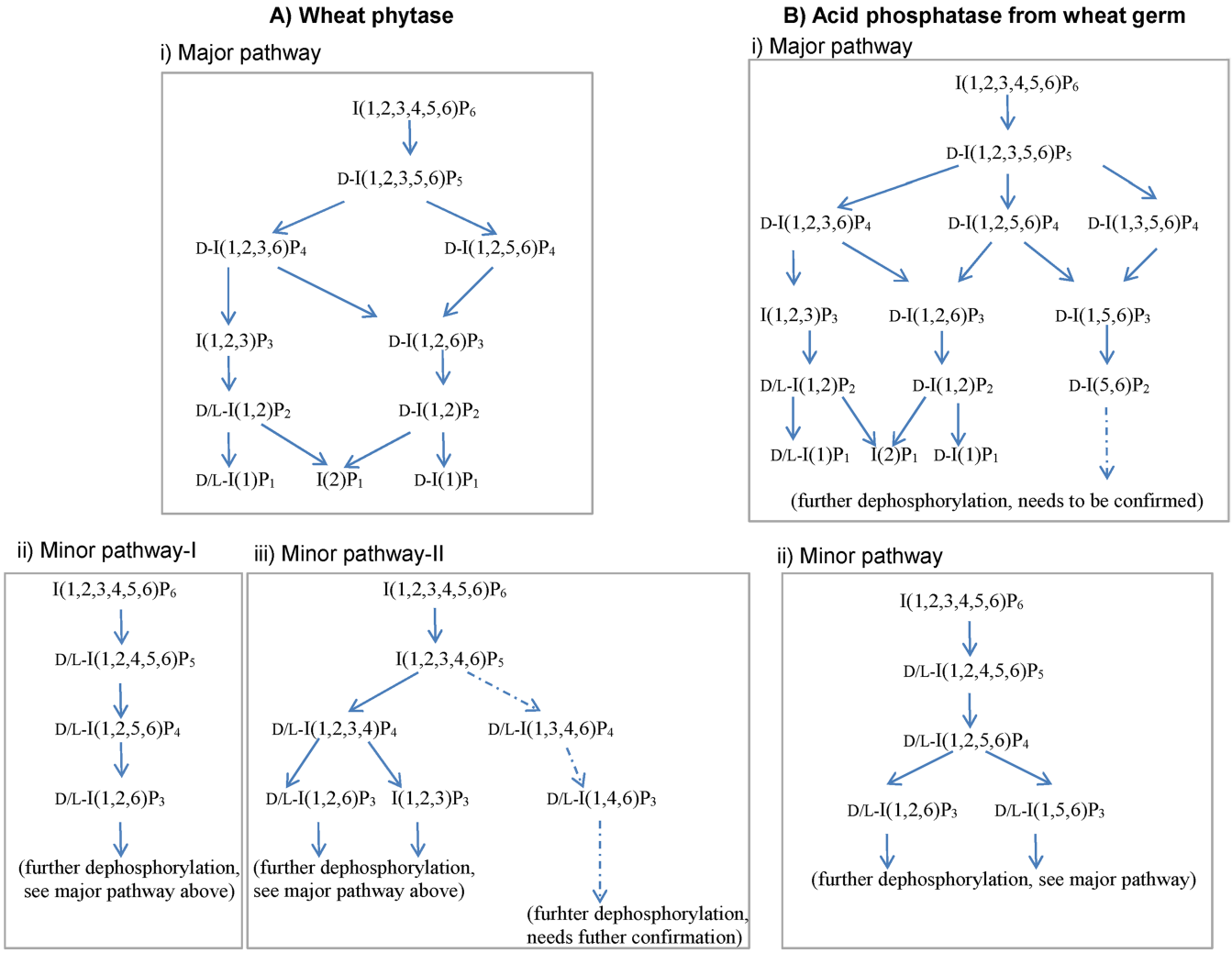

Fig. 8. Possible degradation pathways of phytate catalyzed by (A) wheat phytase and (B) acid phosphatase from wheat germ. Solid arrows refer to confirmed pathways and dashed arrows represent pathways that need further confirmation.

D-I(1,2,5,6)P_4 was the most dominant isomer and appeared for a longer time during degradation. For the minor pathway, D/L-I(1,2,4,5,6)P_5 was further dephosphorylated and formed a series of IP_x isomers. Interestingly, two IP_2 isomers, D/L-I(1,2)P_2 and D/L-I(4,5)P_2 [equivalent to D/L-I(5,6)P_2] generated by acid phosphatase (wheat germ), were different from only one IP_2 isomer, D/L-I(1,2)P_2 generated from wheat phytase. This might potentially be due to some other unknown enzymes present in the acid phosphatase preparation from wheat germ. Nonetheless, the final products generated for this enzyme were identical to those of wheat phytase as I(2)P_1 and D/L-I(1)P_1.

Aspergillus niger phytase is considered a 3-phytase (Greiner et al., 2009). Therefore, the major IP_5 product D/L-I(1,2,4,5,6)P_5 should be D-I(1,2,4,5,6)P_5, with the first dephosphorylation at the C-3 position (Fig. 9A). This IP_5 was further degraded into two IP_4 isomers, D-I(1,2,4,5)P_4 and D-I(1,2,5,6)P_4, with the latter as the dominant isomer. The D-I(1,2,5,6)P_4 could then be dephosphorylated at the C-5 position to generate D-I(1,2,6)P_3. Three IP_3 isomers generated produced a relatively common IP_2 [D-I(1,2)P_2], which finally formed I(2)P_1 and D-I(1)P_1. Low concentrations of I(1,3,4,5,6)P_5 and D/L-I(1,2,3,4,5)P_5 isomers present at the beginning stage of degradation suggested two minor degradation pathways, which are rather complicated due to a series of IP_4 and IP_3 isomers concurrently present. In summary, *A. niger* phytase breaks down phytate mainly from the C-3 position, but might also start from C-4 and C-2 positions to generate D/L-I(1,2,3,5,6)P_5 and I(1,3,4,5,6)P_5 isomers (Fig. 9A). According to Greiner et al. (2009), pure *A. niger* phytase is a rather specific phosphatase and degrades phytate stepwise via D-I(1,2,4,5,6)P_5, D-I(1,2,5,6)P_4, D-I(1,2,6)P_3, D-I(1,2)P_2, and finally to I(2)P_1. One possible reason for the presence of three degradation pathways instead of one might be the fact that the *A. niger* phytase used in this study was a commercial enzyme and was used without purification. It could contain some other unspecified IP_x–active phosphatase enzymes. Another possibility is that the small amounts of D/L-I(1,2,3,5,6)P_5 and I(1,3,4,5,6)P_5 isomers were present as impurities in the original phytate stock, although these products were not noticed at the onset of degradation. If present, these two IP_5 isomers could be further dephosphorylated by *A. niger* phytase.

For acid phosphatase from potato, the phytate degradation pathway was much different and straightforward than those for

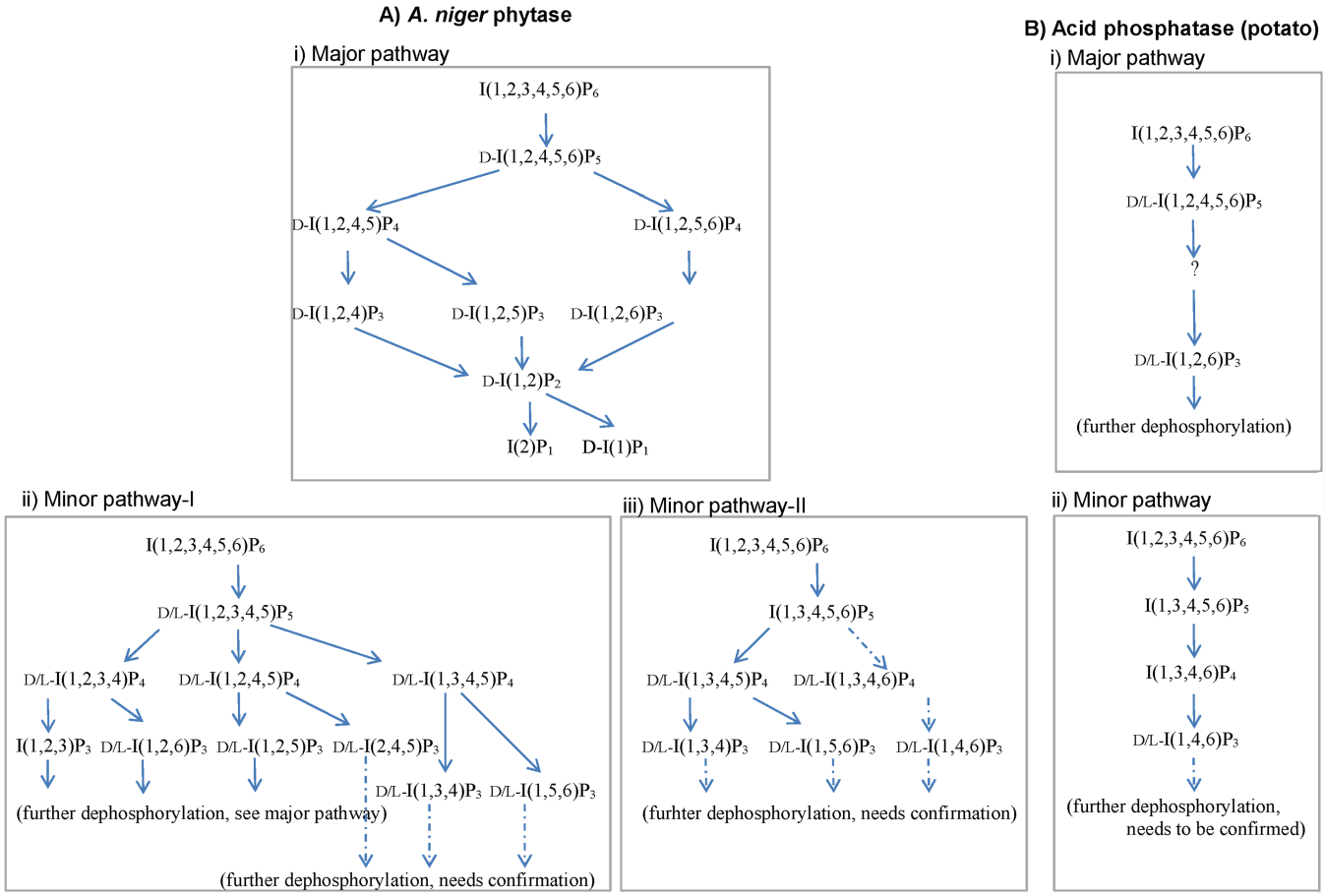

Fig. 9. Possible degradation pathways of phytate catalyzed by (A) *Aspergillus niger* phytase and (B) acid phosphatase from potato. Solid arrows refer to confirmed pathways and dashed arrows represent pathways that need further confirmation.

the other enzymes (Fig. 9B). In short, the minor pathway follows $I(1,3,4,5,6)P_5$ dephosphorylated into $I(1,3,4,6)P_4$, which then generates D/L-$I(1,4,6)P_3$. However, it is difficult to speculate how D/L-$I(1,2,4,5,6)P_5$ in the major degradation pathway was further dephosphorylated. Some studies have found that the glucose phosphatase from *E. coli* and *Pantoea agglomerans* could degrade phytate and generate D-$I(1,2,4,5,6)P_5$ as the final product (Cottrill et al., 2002; Greiner, 2004). Thus one possibility could be that D/L-$I(1,2,4,5,6)P_5$ was generated by a similar enzyme to the *E. coli* and *P. agglomerans* glucose phosphatase as a final product, but it was then further dephosphorylated by an unknown contaminant phosphatase enzyme, perhaps very slowly, to IP_4. The generated IP_4 isomer, however, was short lived (as it was too low to be detected by HPIC) and dephosphorylated quickly to IP_3.

In summary, the four different phytate-degrading enzymes studied provided potential major and minor pathways of phytate degradation. A combination of highly specific methods for inositol phosphate identification, particularly HPIC and NMR, allowed precise identification of isomers. The distinction on structural or positional preference for enzymatic hydrolysis allowed determination of the approximate contribution of particular enzymes as well as the contrast with other enzymes on the stepwise dephosphorylation of inositol phosphates.

Kinetic Rate Estimation

The model result was able to capture the trend and magnitude of the measured concentrations for three enzymes (Fig. 6). This indicates that the developed models (Eq. [3a–3d]) are sufficient to capture the degradation kinetics. In particular, the enzyme-limiting model was able to capture the delay in the beginning of the lower order inositol phosphate degradation. The results of the inverse modeling suggest that the initial enzyme concentration is a limiting factor that controls the rate of decay. This conclusion is also evident from the often constant slopes of the decreasing limbs of the IP curves vs. time. No clear correlation between the reaction rate constants and the order of IP_x molecules, however, was evident.

Isotope Effect: Potential Proxy for Discriminating Enzymes as Well as Sources of Phytate

During enzymatic hydrolysis of phytate, O-isotope values of O in the reactants undergoing nucleophilic attack on a P–O bond with O incorporated into the released PO_4 are different from ambient water O. This difference causes isotope fractionation. Interestingly, this fractionation is specific to the enzyme and substrate type and thus is different (Jaisi et al., 2014; Liang and Blake, 2006, 2009). Whether H_2O, the OH ion, an OH radical, or their different combinations attack a P–O bond and impact isotope fractionation are in the early phase of investiga-

tion for different organic P compounds (Jaisi et al., 2016). On the other hand, the effect of progressive degradation of a natural organophosphorus compound that has several phosphate moieties on isotope fractionation is still unknown, although it is expected to be similar to a synthetic equivalent (Wu et al., 2015). Given that five out of six phosphate groups at different positions of the inositol ring are hydrolyzed by enzymes in a specified sequence (see above and Fig. 8 and 9), any temporal variation of $\delta^{18}O_p$ values would indicate a different isotope composition of the original phosphate moieties at the corresponding structure in the inositol. No significant difference in $\delta^{18}O_p$ values for a particular enzyme, irrespective of variable reaction rates for different isomers at different stages, indicated that all the phosphate moieties released from the phytate ring probably have the same isotope compositions. This finding is valid for both natural and synthetic phytates.

For all enzymes studied, the fractionation factors (F) were all positive (Table 5), which are consistent or similar with published results (von Sperber et al., 2015; Wu et al., 2015). This indicates that the heavy ^{18}O is preferentially incorporated into released P_i during enzymatic degradation of phytate by all four enzymes. The similar positive fractionation factors among the four enzymes could reflect comparable reaction mechanisms, but still the values of F for each enzyme were distinctly different. This could be useful to differentiate the active enzymes for phytate degradation. Because a wide range of fractionation factors have been reported for different substrates as well as enzymes (Liang and Blake, 2006, 2009; von Sperber et al., 2014, 2015), one of the most useful findings that has larger environmental implications is that different enzymes have particular selectivity for phytate degradation and each enzyme has a distinctly different fractionation factor. This distinction opens up the possibility of identifying active phosphohydrolase enzyme(s) responsible for phytate degradation in the environment.

CONCLUSIONS AND IMPLICATIONS

In this research, phytate was hydrolyzed by wheat and *A. niger* phytases and acid phosphatase (from wheat germ and potato), common enzymes present in the environment. On analytical grounds, the combination of HPIC and NMR provided identification of a series of isomers from IP_5 to IP_1 and increased the realm of differentiating products. The distinct degradation products and degradation pathways as well as distinct kinetic decay rates among the enzymes studied provides the possibility of identifying active phytate-degrading enzymes in the environment. Furthermore, the O-isotope compositions of phosphate moieties in the inositol ring are the same. This expands the potential application of O-isotope signatures to identify the original source of phytate from its partially dephosphorylated products in the environment. Furthermore, the fractionation factors among enzymes are different. This also can aid in differentiating active enzymes in the environment. In all, these research findings have important implications for tracking phytate P sources and the overall role in P cycling in the environment.

ACKNOWLEDGMENTS

This work was supported by an NSF grant (EAR 1654642) and USDA grants (NIFA Awards 2013-67019-21373 and 2015-67020-23603). We are grateful to Angelia Seyfferth for access to the HPIC facility for isomer analyses and Yu- Sung Wu of the Protein Production Core Facility at the Delaware Biotechnology Institute for wheat phytase purification (supported by Grant P30 GM103519).

REFERENCES

Adeola, O., J.S. Sands, P.H. Simmins, and H. Schulze. 2004. The efficacy of an *Escherichia coli*-derived phytase preparation. J. Anim. Sci. 82:2657–2666. doi:10.2527/2004.8292657x

Alikhani, J., I. Takacs, A. Al Omari, S. Murthy, and A. Massoudieh. 2017. Evaluation of the information content of long-term wastewater characteristics data in relation to activated sludge model parameters. Water Sci. Technol. (in press). doi:10.2166/wst.2017.004

Barrientos, L., J.J. Scott, and P.P.N. Murthy. 1994. Specificity of hydrolysis of phytic acid by alkaline phytase from lily pollen. Plant Physiol. 106:1489–1495. doi:10.1104/pp.106.4.1489

Blum-Held, C., P. Bernard, and B. Spiess. 2001. *myo*-Inositol 1,4,5,6-tetrakisphosphate and *myo*-inositol 3,4,5,6-tetrakisphosphate, two second messengers that may act as pH-dependent molecular switches. J. Am. Chem. Soc. 123:3399–3400. doi:10.1021/ja015616i

Brejnholt, S.M., G. Dionisio, V. Glitsoe, L.K. Skov, and H. Brinch-Pedersen. 2011. The degradation of phytate by microbial and wheat phytases is dependent on the phytate matrix and the phytase origin. J. Sci. Food Agric. 91:1398–1405. doi:10.1002/jsfa.4324

Celi, L., and E. Barberis. 2007. Abiotic reactions of inositol phosphates in soil. In: B.L. Turner et al., editors, Inositol phosphates: Linking agriculture and the environment. CAB Int., Oxford, UK. p. 207–220. doi:10.1079/9781845931520.0207

Chen, Q.-C., and B.W. Li. 2003. Separation of phytic acid and other related inositol phosphates by high-performance ion chromatography and its applications. J. Chromatogr. A 1018:41–52. doi:10.1016/j.chroma.2003.08.040

Cohn, M., and H.C. Urey. 1938. Oxygen exchange reactions of organic compounds and water. J. Am. Chem. Soc. 60:679–687. doi:10.1021/ja01270a052

Cosgrove, D.J., and G.C.J. Irving. 1980. Inositol phosphates: Their chemistry, biochemistry, and physiology. Elsevier, Amsterdam.

Cottrill, M.A., S.P. Golovan, J.P. Phillips, and C.W. Forsberg. 2002. Inositol phosphatase activity of the *Escherichia coli agp*-encoded acid glucose-1-phosphatase. Can. J. Microbiol. 48:801–809. doi:10.1139/w02-076

Dao, T.H. 2007. Ligand effects on inositol phosphate solubility and bioavailability in animal manures. In: B.L. Turner et al., editors, Inositol phosphates: Linking agriculture and the environment. CAB Int., Oxford, UK. p. 169–185. doi:10.1079/9781845931520.0169

Gerke, J. 2015. Phytate (inositol hexakisphosphate) in soil and phosphate acquisition from inositol phosphates by higher plants: A review. Plants 4:253–266. doi:10.3390/plants4020253

Giles, C.D., and B.J. Cade-Menun. 2014. Phytate in animal manure and soils: Abundance, cycling and bioavailability. In: Z. He and H. Zhang, editors, Applied manure and nutrient chemistry for sustainable agriculture and environment. Springer, New York. p. 163–190. doi:10.1007/978-94-017-8807-6_9

Greiner, R. 2004. Purification and properties of a phytate-degrading enzyme from *Pantoea agglomerans*. Protein J. 23:567–576. doi:10.1007/s10930-004-7883-1

Greiner, R. 2007. Phytate-degrading enzymes: Regulation of synthesis in microorganisms and plants. In: B.L. Turner et al., editors, Inositol phosphates: Linking agriculture and the environment. CAB Int., Oxford, UK. p. 78–96. doi:10.1079/9781845931520.0078

Greiner, R., and M.L. Alminger. 2001. Stereospecificity of *myo*-inositol hexakisphosphate dephosphorylation by a phytate-degrading enzyme of cereals. J. Food Biochem. 25:229–248. doi:10.1111/j.1745-4514.2001.

tb00736.x
Greiner, R., N.-G. Carlsson, and M.L. Alminger. 2000. Stereospecificity of *myo*-inositol hexakisphosphate dephosphorylation by a phytate-degrading enzyme of *Escherichia coli*. J. Biotechnol. 84:53–62. doi:10.1016/S0168-1656(00)00331-X
Greiner, R., L.G. da Silva, and S. Couri. 2009. Purification and characterization of an extracellular phytase from *Aspergillus niger* 11T53A9. Braz. J. Microbiol. 40:795–807. doi:10.1590/S1517-83822009000400010
Greiner, R., E. Haller, U. Konietzny, and K.-D. Jany. 1997. Purification and characterization of a phytase from *Klebsiella terrigena*. Arch. Biochem. Biophys. 341:201–206. doi:10.1006/abbi.1997.9942
Greiner, R., and U. Konietzny. 2011. Phytases: Biochemistry, enzymology and characteristics relevant to animal feed use. In: M.R. Bedford and G.G. Partridge, editors, Enzymes in farm animal nutrition. CAB Int., Oxford, UK. p. 96–128.
Greiner, R., U. Konietzny, and K.D. Jany. 1998. Purification and properties of a phytase from rye. J. Food Biochem. 22:143–161. doi:10.1111/j.1745-4514.1998.tb00236.x
Greiner, R., U. Konietzny, and K.D. Jany. 2006. Phytate: An undesirable constituent of plant-based foods? J. Ernaehrungsmed. 8:18–28.
Irvine, R.F., and M.J. Schell. 2001. Back in the water: The return of the inositol phosphates. Nat. Rev. Mol. Cell Biol. 2:327–338. doi:10.1038/35073015
Jaisi, D.P., and R.E. Blake. 2014. Advances in using oxygen isotope ratios of phosphate to understand phosphorus cycling in the environment. Adv. Agron. 125:1–53. doi:10.1016/B978-0-12-800137-0.00001-7
Jaisi, D.P., R.E. Blake, Y. Liang, and S.J. Chang. 2014. Investigation of compound-specific organic–inorganic phosphorus transformation using stable isotope ratios in phosphate. In: Z. He and H. Zhang, editors, Applied manure and nutrient chemistry for sustainable agriculture and environment. Springer, New York. p. 267–292. doi:10.1007/978-94-017-8807-6_13
Jaisi, D.P., H. Li, A.F. Wallace, P. Paudel, M. Sun, A. Balakrishna, and R. Lerch. 2016. Mechanisms of bond cleavage during Mn oxide and UV degradation of glyphosate: Results from phosphate oxygen isotopes and molecular simulations. J. Agric. Food Chem. 64:8474–8482. doi:10.1021/acs.jafc.6b02608
Konietzny, U., and R. Greiner. 2002. Molecular and catalytic properties of phytate-degrading enzymes (phytases). Int. J. Food Sci. Technol. 37:791–812. doi:10.1046/j.1365-2621.2002.00617.x
Liang, Y., and R.E. Blake. 2006. Oxygen isotope signature of P_i regeneration from organic compounds by phosphomonoesterases and photooxidation. Geochim. Cosmochim. Acta 70:3957–3969. doi:10.1016/j.gca.2006.04.036
Liang, Y., and R.E. Blake. 2009. Compound- and enzyme-specific phosphodiester hydrolysis mechanisms revealed by $d^{18}O$ of dissolved inorganic phosphate: Implications for marine P cycling. Geochim. Cosmochim. Acta 73:3782–3794. doi:10.1016/j.gca.2009.01.038
Lim, P.E., and M.E. Tate. 1973. The phytases: II. Properties of phytase fractions F_1 and F_2 from wheat bran and the *myo*-inositol phosphates produced by fraction F_2. Biochim. Biophys. Acta, Enzymol. 302:316–328.
Lott, J.N.A., I. Ockenden, V. Raboy, and G.D. Batten. 2000. Phytic acid and phosphorus in crop seeds and fruits: A global estimate. Seed Sci. Res. 10:11–33.
McKelvie, I.D. 2007. Inositol phosphates in aquatic systems. In: B.L. Turner et al., editors, Inositol phosphates: Linking agriculture and the environment. CAB Int., Oxford, UK. p. 261–277. doi:10.1079/9781845931520.0261
McLaughlin, K., M.B. Young, A. Paytan, and C. Kendall. 2013. The oxygen isotopic composition of phosphate: A tracer for phosphate sources and cycling. In: Application of isotope techniques for assessing nutrient dynamics in river basins. IAEA-TECDOC-1695. Int. Atomic Energy Agency, Vienna. p. 93–110.
Meek, J.L., and F. Nicoletti. 1986. Detection of inositol trisphosphate and other organic phosphates by high-performance liquid chromatography using an enzyme-loaded post-column reactor. J. Chromatogr. A 351:303–311. doi:10.1016/S0021-9673(01)83500-7
Mullaney, E.J., A.H.J. Ullah, B. Turner, A. Richardson, and E. Mullaney. 2007. Phytases: Attributes, catalytic mechanisms and applications. In: B.L. Turner et al., editors, Inositol phosphates: Linking agriculture and the environment. CAB Int., Oxford, UK. p. 97–110. doi:10.1079/9781845931520.0097
Murphy, J., and J.P. Riley. 1962. A modified single solution method for the determination of phosphate in natural waters. Anal. Chim. Acta 27:31–36. doi:10.1016/S0003-2670(00)88444-5
Nagai, Y., and S. Funahashi. 1962. Phytase (*myo*-inositolhexaphosphate phosphohydrolase) from wheat bran: I. Purification and substrate specificity. Agric. Biol. Chem. 26:794–803.
Nakano, T., T. Joh, K. Narita, and T. Hayakawa. 2000. The pathway of dephosphorylation of *myo*-inositol hexakisphosphate by phytases from wheat bran of *Triticum aestivum* L. cv. Nourin #61. Biosci. Biotechnol. Biochem. 64:995–1003. doi:10.1271/bbb.64.995
Raboy, V. 1997. Accumulation and storage of phosphate and minerals. In: B.A. Larkins and I.K. Vasil, editors, Cellular and molecular biology of plant seed development. Springer, New York. p. 441–477. doi:10.1007/978-94-015-8909-3_12
Shan, Y., I.D. McKelvie, and B.T. Hart. 1993. Characterization of immobilized *Escherichia coli* alkaline phosphatase reactors in flow injection analysis. Anal. Chem. 65:3053–3060. doi:10.1021/ac00069a018
Shears, S.B., and B.L. Turner. 2007. Nomenclature and terminology of inositol phosphates: Clarification and a glossary of terms. In: B.L. Turner et al., editors, Inositol phosphates: Linking agriculture and the environment. CAB Int., Oxford, UK. p. 1–6. doi:10.1079/9781845931520.0001
Turner, B.L., and S. Newman. 2005. Phosphorus cycling in wetland soils. J. Environ. Qual. 34:1921–1929. doi:10.2134/jeq2005.0060
Turner, B.L., M.J. Papházy, P.M. Haygarth, and I.D. McKelvie. 2002. Inositol phosphates in the environment. Philos. Trans. R. Soc. London, Ser. B 357:449–469. doi:10.1098/rstb.2001.0837
Upreti, K., S.R. Joshi, J. McGrath, and D.P. Jaisi. 2015. Factors controlling phosphorus mobilization in a Coastal Plain tributary to the Chesapeake Bay. Soil Sci. Soc. Am. J. 79:826–837. doi:10.2136/sssaj2015.03.0117
von Sperber, C., H. Kries, F. Tamburini, S.M. Bernasconi, and E. Frossard. 2014. The effect of phosphomonoesterases on the oxygen isotope composition of phosphate. Geochim. Cosmochim. Acta 125:519–527. doi:10.1016/j.gca.2013.10.010
von Sperber, C., F. Tamburini, B. Brunner, S.M. Bernasconi, and E. Frossard. 2015. The oxygen isotope composition of phosphate released from phytic acid by the activity of wheat and *Aspergillus niger* phytase. Biogeosciences 12:4175–4184. doi:10.5194/bg-12-4175-2015
Wu, J., P. Paudel, M. Sun, S.R. Joshi, L.M. Stout, R. Greiner, and D.P. Jaisi. 2015. Mechanisms and pathways of phytate degradation: Evidence from oxygen isotope ratios of phosphate, HPLC, and phosphorus-31 NMR spectroscopy. Soil Sci. Soc. Am. J. 79:1615–1628. doi:10.2136/sssaj2015.01.0002
Wyss, M., R. Brugger, A. Kronenberger, R. Rémy, R. Fimbel, G. Oesterhelt, et al. 1999. Biochemical characterization of fungal phytases (*myo*-inositol hexakisphosphate phosphohydrolases): Catalytic properties. Appl. Environ. Microbiol. 65:367–373.